Antiviral Research 93 (2012) 270–279

Contents lists available at SciVerse ScienceDirect

Antiviral Research

journal homepage: www.elsevier.com/locate/antiviral

MiR-342-5p suppresses coxsackievirus B3 biosynthesis by targeting the 2C-coding region

Linlin Wang [a,c,1], Ying Qin [a,1], Lei Tong [a], Shuo Wu [a], Qiang Wang [a], Qingguo Jiao [a], Zhiwei Guo [a], Lexun Lin [a], Ruixue Wang [a], Wenran Zhao [b,*], Zhaohua Zhong [a,*]

[a] Department of Microbiology, Harbin Medical University, Harbin 150081, China
[b] Department of Cell Biology, Harbin Medical University, Harbin 150081, China
[c] Department of Laboratory Diagnosis, The First Hospital of Harbin Medical University, Harbin 150001, China

ARTICLE INFO

Article history:
Received 12 October 2011
Revised 6 December 2011
Accepted 7 December 2011
Available online 13 December 2011

Keywords:
MiR-342-5p
Coxsackievirus B3
Biosynthesis
2C-coding region
Antiviral activity

ABSTRACT

Coxsackievirus B type 3 (CVB3) is one of the major pathogens associated with human heart disease. miRNAs are a class of short, noncoding RNA that can post-transcriptionally modulate gene expression. By comparing the CVB3 genome and miR-342-5p sequences, we found there were potential miR-342-5p targets in the CVB3 genome. To verify the effect of miR-342-5p on CVB3 biosynthesis, HeLa cells were infected with a *Renilla* luciferase (RLuc)-expressing CVB3 variant (RLuc-CVB3). We observed that miR-342-5p could significantly inhibit the expression of RLuc in infected cells. In HeLa cells infected with an enhanced green fluorescence protein (EGFP)-expressing CVB3 variant (EGFP-CVB3), EGFP expression was also significantly inhibited by miR-342-5p. The inhibitory effect of miR-342-5p on EGFP expression in EGFP-CVB3-infected cells could be reversed by transfection with anti-miR-342-5p oligonucleotide (AMO-miR-342-5p). Moreover, RNA and protein biosynthesis in wild-type CVB3 was significantly inhibited by miR-342-5p. By mutating the putative targets of miR-342-5p in the 2C-coding region, a sequence, nt4989–nt5015, was identified as the miR-342-5p target. The conserved nt4989–nt5015 sequences of CVB type 1–5 suggest miR-342-5p may exert its inhibitory effect in other types of coxsackievirus besides CVB3. Western blotting indicated that miR-342-5p could indeed suppress protein expression in CVB type 1 and 5. There was a moderate abundance of miR-342-5p in the gut, heart, and brain of Balb/c mice, suggesting that miR-342-5p may interact with CVB3 *in vivo*. Taken together, these results indicate that miR-342-5p can inhibit CVB3 biosynthesis by targeting its 2C-coding region and therefore may be a potential therapeutic agent in the treatment of CVB3 infection.

1. Introduction

Enterovirus-caused diseases are a major health problem worldwide. Among the enteroviruses, coxsackievirus is involved in a wide range of human diseases, especially in neonates and children. Severe health consequences have been associated with outbreaks of coxsackievirus infection (Cui et al., 2010a; Verma et al., 2009; Wong et al., 2011). Moreover, group B coxsackievirus (CVB) infection has been implicated in the development of myocarditis and dilated cardiomyopathy (Bowles et al., 1986; Jin et al., 1990; Knowlton, 2008; Martin et al., 1994; Tracy et al., 1990). In spite of this, there is presently no specific and effective therapy available for CVB infection.

MicroRNAs (miRNAs) are a class of small RNAs 20–23 nucleotides (nt) in length that are found in almost all eukaryotic cells. miRNAs play an important role in the post-transcriptional regulation of gene expression (Ambros, 2004; Asli et al., 2008; Bartel, 2004). Generally, miRNAs suppress the translation of target genes through imperfect binding to target sequences in animal-cell mRNA or promote mRNA degradation through perfect binding to target sequences in plant-cell mRNA (Ambros, 2004; Bartel, 2004). Due to their crucial role in post-transcriptional regulation of gene expression, miRNAs are involved in many important biological processes including development, cell differentiation, cell proliferation, apoptosis, and a variety of disease states (Ambros, 2004; Asli et al., 2008; Bartel, 2004; Esquela-Kerscher and Slack, 2006; Kloosterman and Plasterk, 2006). miRNAs have also been implicated in the pathology of diseases caused by viruses such as hepatitis viruses, human immunodeficiency virus, and herpes viruses (Jiang et al., 2008; Lecellier et al., 2005; Pedersen et al., 2007; Sullivan and Ganem, 2005). Thus, miRNAs play pivotal roles in the regulation of gene expression of both viruses and host cells.

* Corresponding authors. Tel.: +86 451 86612713 (W. Zhao), tel./fax: +86 451 86685122 (Z. Zhong).
E-mail addresses: wenran.zhao@gmail.com (W. Zhao), zhongzh@hrbmu.edu.cn (Z. Zhong).
[1] These authors equally contributed to this work.

0166-3542/$ - see front matter © 2011 Elsevier B.V. All rights reserved.
doi:10.1016/j.antiviral.2011.12.004

As members of the *Picornaviridae* family, the CVBs are single-stranded positive-sense RNA viruses. Their genomic RNA can work directly as mRNA to guide protein biosynthesis in host cells (Bedard and Semler, 2004). Therefore, it is rational to assume that picornaviruses can be regulated by cellular miRNAs. Indeed, a simulation study has demonstrated, by artificially modification of the 3′ untranslated region (3′ UTR) of coxsackievirus A21 to incorporate miR-142 targets, that miR-142 can interrupt the life cycle of coxsackievirus A21 in multiple steps, including degradation of the viral genome, suppression of cap-independent mRNA translation, and interference with genome encapsidation (Kelly et al., 2010). On the other hand, picornavirus infections can also evoke or suppress the expression of particular cellular miRNAs (Cui et al., 2010b). For example, miR-141 expression can be upregulated upon enterovirus infection, helping both to shut off host protein synthesis and facilitate virus propagation by targeting the cap-dependent translation initiation factor, eIF4E (Ho et al., 2011). However, so far, there are no available data on the interactions between cellular miRNAs and CVB replication.

In the present study, we found that miR-342-5p could specifically suppress CVB3 biosynthesis and replication through the targeting of the 2C-coding sequence of the CVB3 genome. Our results suggest that miR-342-5p may be a potential therapeutic agent for the treatment of CVB3 infection.

2. Materials and methods

2.1. miRNA target prediction

CVB3 genome miRNA targets were predicted by RNAhybrid 2.2 (bibiserv.techfak.uni-bielefeld.de/rnahybrid) and miRanda 3.2a (www.microrna.org). The potential binding sites were selected by choosing the complementary base sequences with minimum free energy (mfe) (Alves et al., 2009; Rajewsky, 2006).

2.2. Cells and mice

HeLa cells were cultured in Dulbecco Modified Eagle Medium (DMEM) (Invitrogen, Carlsbad, CA) supplemented with 10% (growth medium) or 5% (maintenance medium) fetal bovine serum (FBS) (Biological Industries, Israel) and antibiotics (50 U/ml penicillin and 50 mg/ml streptomycin) at 37 °C with 5% CO_2. Pathogen-free, 2-week-old Balb/c mice were obtained from the Harbin Medical University Experimental Animal Center. The mice were maintained and sacrificed in accordance with the Regulations on the Usage of Experimental Animals of Harbin Medical University.

2.3. Nucleotides and plasmids

The necessary miRNAs, miR-342-5p, control miRNAs, and miR-mock, were synthesized by GenePharma (Shanghai, China) and TaKaRa (Dalian, China). Anti-miR-342-5p oligonucleotide (AMO-miR-342-5p), an oligo-RNA (5′-UCAAUCACAGAUAGCACCCCU-3′) with a 2′-*O*-methoxyethyl group (Weiler et al., 2006), was synthesized by GenePharma. The plasmid pMKS-1, containing the full-length cDNA of the CVB3 genome, was a gift from Professor J. Lindsay Whitton of the Scripps Research Institute, La Jolla, California (Feuer et al., 2002). pMKS-1 was used as a basis to design and construct plasmids containing the entire cDNA sequence of CVB3 genome and a reporter gene, enhanced green fluorescence protein (EGFP) or *Renilla* luciferase (RLuc), which were designated as pEGFP-CVB3 and pRLuc-CVB3, respectively (Tong et al., 2011). pGL4.17, a plasmid expressing firefly luciferase (FLuc), was obtained from Promega (Madison, WI).

Two plasmids, designated as pEGFP-VP4-3 and pEGFP-2C, were constructed to express the CVB3 proteins VP4-VP2-VP3 (VP4-3) and 2C, respectively. Both viral proteins were expressed as fusion proteins with EGFP at the N-terminus. Briefly, the EGFP-coding sequence was amplified via polymerase chain reaction (PCR) from pEGFP-N1 (Clontech, Mountain View, CA) with the sense primer ATATATAGCTAGCATGGTGAGCAAGGGCGAGGAGCT (underlined: *Nhe*I restriction site) and the antisense primer GCTTTAAGCTTCTTGTACAGCTCGTCCATGCCG (underlined: *Hind*III restriction site). Both pcDNA3.1 (Invitrogen) and the amplified EGFP fragment were digested with *Nhe*I and *Hind*III restriction endonucleases and ligated by incubation with T4 ligase at 16 °C overnight. The constructed plasmid was designated as pEGFP-C1. Total RNA was extracted from HeLa cells infected with CVB3 using TRIzol (Invitrogen). Subsequently, 1 μg of total RNA was used for reverse-transcription with antisense primers of target sequences. The VP4-3-coding sequence was amplified with the sense primer ATATATATGGTACCGGTGGAGGCGGTTCAGGCGGAGGTGGCTCTGGCGGTGGCGGATCGGGAGCTCAAGTATCAACGCAAAAGAC (underlined: *Kpn*I restriction site) and the antisense primer GCGCGCTCTAGAATTACTGGAAAAAGTTTTGCTGCGAAATAAAAGGAGTGT (underlined: *Xba*I restriction site). The 2C-coding sequence was amplified with the sense primer ATATATAAGCTTGGTGGAGGCGGTTCAGGCGGAGGTGGCTCTGGCGGTGGCGGATCGAACAACGGATGGCTAAAAAAGTT (underlined: *Hind*III restriction site) and the antisense primer ATAGCGTCTAGATTACTGGAACAGTGCCTCAAGGGTAGCCCCGACAC (underlined: *Xba*I restriction site). The amplified fragments and pEGFP-C1 were digested with *Kpn*I and *Xba*I endonucleases (for VP4-3) or *Hind*III and *Xba*I endonucleases (for 2C). The digested VP4-3 and 2C fragments were separately ligated into the digested pEGFP-C1 at 16 °C overnight. The successful construction of the plasmids was confirmed by restrict digestion and sequencing.

2.4. Viruses

Wild-type CVB3 Woodruff, CVB type 1 (CVB1), and CVB type 5 (CVB5) were cultured in HeLa cells. Two CVB3 variants, EGFP-CVB3 and RLuc-CVB3, were recovered by transfecting HeLa cells with pEGFP-CVB3 and pRLuc-CVB3, respectively. Briefly, HeLa cells were seeded in 12-well culture plates at the density of 1×10^5 cells/well and cultured for 18–24 h. When 60–70% confluence was reached, the cells were transfected with 0.8 μg of pEGFP-CVB3 and pRLuc-CVB3, respectively, and maintained in DMEM with 5% FBS. Cytopathic effects (CPE) in the transfected cells were observed at 24 h post-transfection. The recovered viruses were purified and titered by plaque assay.

2.5. Viral plaque assay

Virus titer was determined by plaque assay as described previously (Yuan et al., 2004; Zhong et al., 2008). Briefly, the viral stock was serially 10-fold diluted in maintenance medium. HeLa cells were seeded in 6-well plates at the density of 2×10^5 cells/well and incubated at 37 °C with 5% CO_2 for 18–24 h. When the cells reached approximately 90% confluency, they were washed with phosphate-buffered saline (PBS) and overlaid with 450 μl of viral diluent. The cells were incubated for 1 h, and the supernatant was removed. Finally, the cells were overlaid with 2 ml of solid medium containing DMEM, 5% FBS, and 0.8% agarose (Promega). The culture plates were incubated in a humidified chamber for 30 min and then inverted. The cells were incubated for another 72 h at 37 °C with 5% CO_2 before being stained with 0.05% neutral red (Sigma, St. Louis, MO) for 1 h. The plaques were counted, and the amount of virus titer (pfu/ml) was calculated.

2.6. RNA transfection

HeLa cells were transfected with miRNAs and AMO-miR-342-5p as described previously (Wu et al., 2009). Briefly, HeLa cells in DMEM with 5% FBS and antibiotics were seeded in 6- to 96-well plates according to the needs of the individual experiments and cultured at 37 °C with 5% CO_2 for 18–24 h. The culture media were removed and replaced by fresh media without antibiotics. Lipofectamine 2000 (Invitrogen) was then used to transfect the miRNAs and AMO-miR-342-5p into the cells. For 96-well plates, 0.2 μl of Lipofectamine 2000 and 0.16 μg of synthetic RNA was diluted with an equal volume of Opti-MEM (Invitrogen), mixed at room temperature for 15 min and then added to each well of the culture plate. The transfected cells were cultured at 37 °C with 5% CO_2 for further study.

2.7. Quantitative reverse-transcription polymerase chain reaction (RT-qPCR)

The total RNA was extracted from HeLa cells or mouse tissues using TRIzol reagent (Invitrogen) as described previously (Wu et al., 2009). After extraction, 1 μg of total RNA was used as template in a reverse transcription along with antisense primers and PrimeScript RT Enzyme Mix I (TaKaRa, Otsu, Shiga, Japan). Quantitative PCR was performed with 1 μl of the synthesized cDNA, SYBR PrimeScript Ex Taq II (TaKaRa), and the sense/antisense primers for a final reaction volume of 20 μl in a LightCycler 2.0 (Roche, Basel, Switzerland). The CVB3 RNA detection primers were GCACACACCC TCAAACCAGA (sense) and ATGAAACACGGACACCCAAAG (antisense). U6 snRNA was used as internal control for quantifying miRNA expression, while GAPDH mRNA was used as the internal control for quantifying viral RNA. The U6 snRNA primers were GCTTCGGCAGCACATATACTAAAAT (sense) and CGCTTCACGAATT TGCGTGTCAT (antisense). The GAPDH mRNA primers were GCACCGTCACGGCTGAGAAC (sense) and TGGTGAAGACGCCAGTGGA (antisense). The $2^{-\Delta\Delta Ct}$ method (Livak and Schmittgen, 2001) was used to calculate the relative levels of miRNAs and viral RNA.

2.8. Luciferase assay

Luciferase activity was measured using a Dual-Luciferase Assay Kit (Promega). Briefly, 70% confluent HeLa cells in 96-well plates were co-transfected with 0.2 μg of miRNA and 0.2 μg of pGL4.17 using Lipofectamine 2000. The transfected cells were infected with 0.1 multiplicity of infection (MOI) of RLuc-CVB3 at 24 h post-transfection. Cell lysates were prepared from the infected cells at 6 h-intervals from 0 to 40 h. The culture medium was removed, and the cells were washed with PBS. Next, 1× Passive Lysis Buffer (Promega) was added to the plates (20 μl/well). The culture plates were placed on a rocking platform for 15 min at room temperature. After rocking, 20 μl of cell lysate and 100 μl of LAR II reagent were thoroughly mixed for 1–2 s. FLuc activity was measured with a Luminometer 20/20^n (Turner BioSystems, Sunnyvale, CA). For FLUC detection, 100 μl of Stop & Glo reagent was added to each well, and RLuc activity was measured. FLuc expression was used as the internal control for normalizing cell population and transfection efficiency. The ratio of RLuc activity to FLuc activity was defined as the relative activity of RLuc in the samples. The experiments were conducted a minimum of three times.

2.9. Quantitation of EGFP expression

EGFP expression in EGFP-CVB3-infected cells (MOI = 0.5) was analyzed at 24–40 h postinfection (p.i.) using fluorescence microscopy (Axiovert 200, Carl Zeiss, Gottingen, Germany), flow cytometry, and fluorescence spectrometry. For flow cytometry, the treated cells were collected at set timepoints. The cells were washed and resuspended in cold PBS. Aliquots of 2×10^5 cells resuspended in 0.2 ml of PBS were used for both cell counting (10,000 cells) and the measurement of fluorescence intensity with a FACSCalibur flow cytometer (BD Biosciences, San Jose, CA). For fluorescence spectrometry, the fluorescent dye Hoechst 33342 (Invitrogen) was added to the culture medium to stain cell nucleus 12–24 h before harvest. The proteins were extracted using Pierce RIPA Buffer (Thermo, Rockford, IL) along with a protease inhibitor phenylmethylsulfonyl fluoride (PMSF) cocktail (Beyotime, Beijing, China). The proteins concentrations were adjusted to the same level (0.25 μg/μl), and 2 μl of proteins were used for fluorescence intensity measurement with a NanoDrop 3300 fluorescent spectrometer (Thermo). The EGFP fluorescence intensity (excitation at 488 nm and emission at 509 nm) was normalized to the Hoechst 33342 fluorescence intensity (excitation at 347 nm and emission at 483 nm) to eliminate variation in the cell populations of each sample.

2.10. Western blot

The proteins from treated HeLa cells were extracted using Pierce RIPA Buffer with PMSF cocktail, and 1–2 μg of extracted proteins were applied to sodium dodecyl sulfate–polyacrylamide gel electrophoresis (SDS–PAGE). The separated proteins were transferred to a polyvinylidene fluoride (PVDF) film (0.45 μm, Millipore, Billerica, Massachusetts) and incubated with primary antibody over night at 4 °C. After a standard washing, the film was incubated with horseradish peroxidase (HRP)-labeled secondary antibody for 1 h at room temperature and washed again. The blots were stained using a SuperSignal kit (Pierce, Rockford, Illinois) and imaged by a charge-coupled camera LAS4000 (Fujifilm, Tokyo, Japan). A monoclonal mouse anti-enterovirus VP1 (clone 5-D8/1) antibody (Dako, Glostrup, Denmark) was used for VP1 detection (1:1000 diluted). β-Actin, a loading control, was detected using a polyclonal antibody (sc-130301) (Santa Cruz Biotechnology, Santa Cruz, CA).

2.11. Site-directed mutagenesis of pEGFP-2C

To mutate the nt4293–nt4321 sequence, pEGFP-2C was amplified with primer pair A (A1: GCGCGCAAGCTTAACAACGGATGGCTA AAAAAGTTCACT, A2: AGGAGCATATTTCCTACAGTAGTGCGCAAAG TATTGGACATTGGA; underlined: *Hind*III restriction site) and primer pair B (B1: GCACTACTGTAGGAAATATGCTCCTCTTTATGCATCAG AGGCAAAGAGAG, B2: ATAGCGTCTAGATTACTGGAACAGTGCCTC; underlined: *Xba*I restriction site), respectively. The resultant products were purified and mixed together. The mixture was denatured and amplified with the primers A1 and B2. The amplified DNA was purified, digested with *Hind* III and *Xba* I, and ligated into pEGFP-C1/*Hind* III + *Xba* I. This plasmid was designated as pEGFP-2C/m1 (Fig. S2). Using the same protocol with primer pair C (A1, C1: GAGCGTCGCACCAACACTATGTCTATGGTTGTATTCCCTAAACATCTCAG) and primer pair D (D1: TAGACATAGTGTTGGTGCGACGCTCGAGG CACTGTTCC, B2), pEGFP-2C/m2 with mutations in the nt4989–nt5015 sequence was generated (Fig. S2). Using pEGFP-2C/m1 as a template, pEGFP-2C/m1 + m2 was generated by repeating amplification, restriction digestion, and ligation for the m2 mutation (Fig. S2). The mutations in these plasmids were verified by DNA sequencing.

2.12. Statistical analysis

Data are presented as the mean ± standard deviation (s.d.). Statistical significance ($P < 0.05$) was determined with Student's *t*-test by SigmapStat 3.1 (Systat Software, Richmond, CA). All experiments were repeated at least three times.

3. Results

3.1. The putative miR-342-5p targets in the CVB3 genome

Upon screening the potential miRNA targets in the CVB3 genome with RNAhybrid 2.2 and miRanda 3.2a (Alves et al., 2009), three putative miR-342-5p targets in the CVB3 genome were identified. These targets were all located in CVB3 open reading frame. Among them, one was located in the VP2-coding region (nt1679–nt1696), while the others resided in the 2C-coding region (nt4293–nt4321 and nt4989–nt5015) (Fig. 1). Although the mfe of the nt1679–nt1696 sequence was the lowest, it was not perfectly matched to the seed sequence of miR-342-5p. Nt4293–nt4321 and nt4989–nt5015 matched the seed sequence of miR-342-5p better but did not have the lowest mfe. Therefore, these possible miR-342-5p targets in the CVB3 genome need verification.

3.2. MiR-342-5p inhibits the biosynthesis of RLuc-CVB3

HeLa cells were employed to study the effects of miR-342-5p on CVB3. First, miR-342-5p abundance in HeLa cells was analyzed to ensure there was no endogenous miR-342-5p that may interfere with our observations. In addition, miR-21 and miR-122 levels were also analyzed in the experiments as controls. Our results indicate there was no endogenous miR-342-5p and miR-122 expression in HeLa cells and that miR-21 was abundant (Fig. S1). The miR-21 and miR-122 expression levels in the HeLa cells were in agreement with previous reports (Ma et al., 2010; Schmittgen et al., 2004). Moreover, no endogenous miR-342-5p expression could be detected in CVB3-infected HeLa cells (data not shown).

To verify the predicted effect of miR-342-5p on CVB3, we introduced miR-342-5p and other randomly selected miRNAs (miR-mock, miR-690, miR-697, miR-412, miR-709, and miR-711) separately into HeLa cells. The pGL4.17 plasmid, which expresses FLuc, was also co-transfected with the miRNAs. The cells were infected with RLuc-CVB3 24 h post-transfection. The RLuc and FLuc luciferase activity levels were measured 24 h p.i., and the relative activity of RLuc was calculated. The RLuc activity in the miR-342-5p-treated cells was significantly lower than that in the cells treated with control miRNAs ($P < 0.01$, $n = 6$) (Fig. 2A), suggesting that miR-342-5p could effectively suppress the biosynthesis of RLuc-CVB3 but other tested miRNAs could not.

Furthermore, continuous examination over a period of 40 h indicated that RLuc activity decreased from 8 to 40 h p.i. in the miR-342-5p-treated HeLa cells infected with RLuc-CVB3. Significant inhibition in RLuc activity was found at 16, 24, and 32 h p.i. ($P < 0.05$, $P < 0.01$, and $P < 0.01$, respectively, $n = 4$) (Fig. 2B). These data further support that miR-342-5p inhibited RLuc-CVB3 biosynthesis.

3.3. MiR-342-5p inhibits the biosynthesis of EGFP-CVB3

To further verify the inhibitory effect of miR-342-5p on CVB3 biosynthesis, HeLa cells were transfected with miR-342-5p or with both miR-342-5p and its inhibitor, AMO-miR-342-5p. The cells were infected with EGFP-CVB3 24 h post-transfection. Under fluorescence microscope, EGFP expression in HeLa cells transfected with miR-342-5p was significantly suppressed, and CPE in these cells was also reduced compared to the CPE observed in cells transfected with miR-mock (Fig. 3A). EGFP expression and CPE in the cells transfected with miR-342-5p increased when AMO-miR-342-5p was introduced (Fig. 3A). A flow cytometric analysis demonstrated that the number of EGFP-positive cells among the miR-342-5p-treated cells (33.3 ± 1.8) was significantly decreased compared to the miR-mock-treated cells (46.1 ± 1.5, $P < 0.05$, $n = 4$) (Fig. 3B). There was no significant difference between the number of EGFP-positive cells among the cells treated with both miR-342-5p and AMO-miR-342-5p (42.1 ± 1.4) and among the cells treated with miR-mock ($P > 0.05$, $n = 4$) (Fig. 3B). Moreover, the fluorescence intensities were consistent with that of EGFP-positive cell counts (Fig. 3C). These data indicate that miR-342-5p could also suppress the biosynthesis of EGFP-CVB3.

3.4. MiR-342-5p inhibits wild-type CVB3 biosynthesis

RLuc-CVB3 and EGFP-CVB3 are artificially modified variants. They may not be fully reflective of wild-type CVB3. Therefore, the effects of miR-342-5p on wild-type CVB3 (Woodruff strain) were also evaluated in this study. Viral infection and transfection was performed according to the same protocols described above. RT-qPCR detection indicated genomic RNA replication of CVB3 was significantly inhibited in the cells treated with miR-342-5p compared to miR-mock-treated cells ($P < 0.01$, $n = 6$) (Fig. 4A). The inhibition could be reversed by treatment with

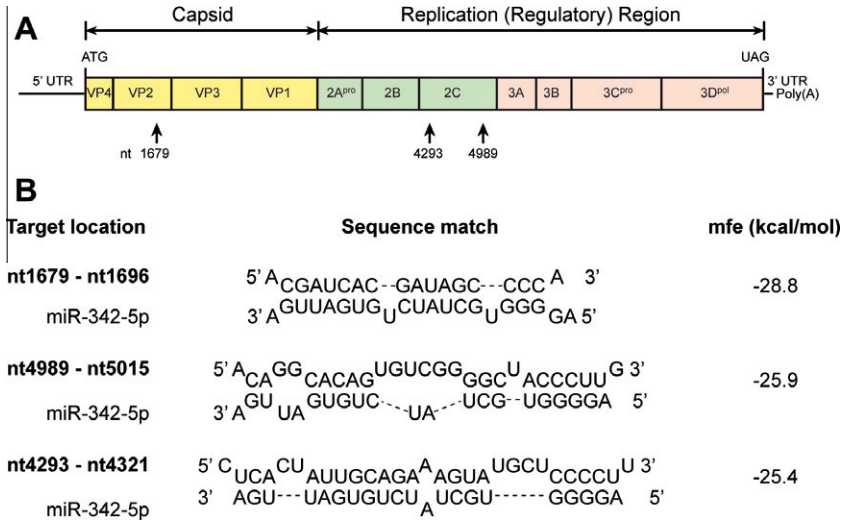

Fig. 1. CVB3 genome miR-342-5p target predictions. (A) The genomic structure of CVB3. The locations of these putative targets are marked by arrows. (B) The matching sequences of miR-342-5p in the CVB3 genome in order of minimum free energy (mfe). "nt" stands for nucleotide, the number counts from the first nucleotide at the 5′ end of the CVB3 genome (GenBank accession: U57056).

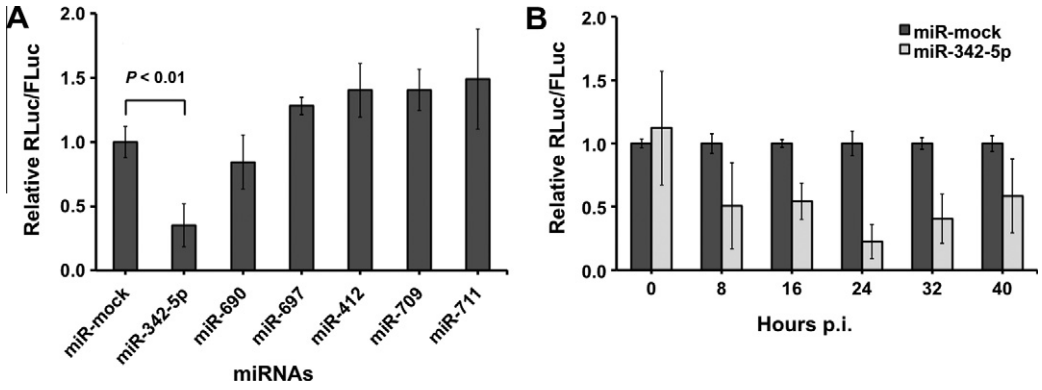

Fig. 2. Inhibitory effect of miR-342-5p on the biosynthesis of RLuc-CVB3. (A) Confluent HeLa cells in 96-well plates were co-transfected with various miRNAs and pGL4.17. The transfected cells were infected with RLuc-CVB3 (MOI = 0.1) 24 h post-transfection. The RLuc and FLuc luciferase activities were measured 24 h p.i. with dual luciferase reagents. Results are presented as the mean ± s.d. (n = 6). (B) Confluent HeLa cells were identically treated as above, and the activities of RLuc and FLuc were measured at 8 h-intervals from 0 to 40 h p.i. RLuc activity was first normalized to FLuc activity to remove the variation of transfection efficiency and cell population. The RLuc/Fluc ratio of each treatment group was further normalized to that of miR-mock-treated cells. Error bars represent the s.d. (n = 4).

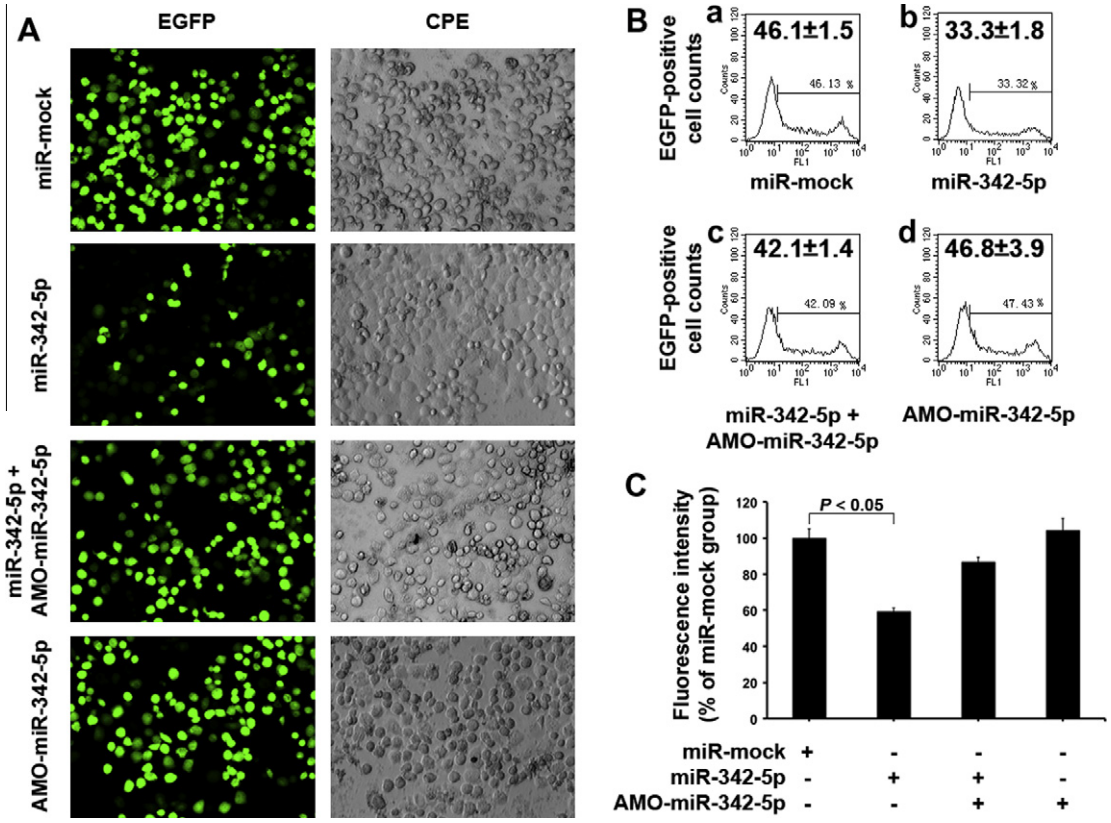

Fig. 3. Inhibitory effect of miR-342-5p on the biosynthesis of EGFP-CVB3. HeLa cells transfected with miR-342-5p or with both miR-342-5p and AMO-miR-342-5p. Cells were infected with EGFP-CVB3 (MOI = 0.5) 24 h post-transfection. (A) Cytopathic effects were observed at 32 h p.i. under fluorescence microscope (200×). (B and C) EGFP-positive cell counts (B) and green fluorescence intensity (C) were measured using a FACSCalibur at 32 h p.i. Error bars represent the s.d. (n = 4).

AMO-miR-342-5p, which increased CVB3 RNA expression almost to the levels observed in miR-mock-treated cells ($P > 0.05$, n = 6) (Fig. 4A). Western blotting indicated that the expression of CVB3 VP1 protein was also apparently inhibited by miR-342-5p in the infected HeLa cells, while the VP1 expression increased in CVB3-infected cells treated with miR-342-5p and AMO-miR-342-5p together (Fig. 4B). These results indicate that the effect of miR-342-5p on wild-type CVB3 was consistent with the effects observed using RLuc-CVB3 and EGFP-CVB3. In addition, miR-342-5p both suppressed the protein biosynthesis of CVB3 and inhibited the CVB3 genomic expression.

3.5. MiR-342-5p suppresses CVB3 biosynthesis by targeting the 2C-coding region

To validate the predicted miR-342-5p CVB3 genomic targets, the VP4-VP2-VP3-coding region (VP4-3) and the 2C-coding region of the CVB3 genome were cloned and fused with an EGFP-coding sequence at the 5′ ends of the viral sequences. The sequences coding the fusion proteins were inserted into the multi-cloning site of the eukaryotic expression vector pcDNA3.1. The constructed plasmids, pEGFP-VP4-3 and pEGFP-2C, were used to co-transfect HeLa cells with miR-342-5p. EGFP expression was determined by

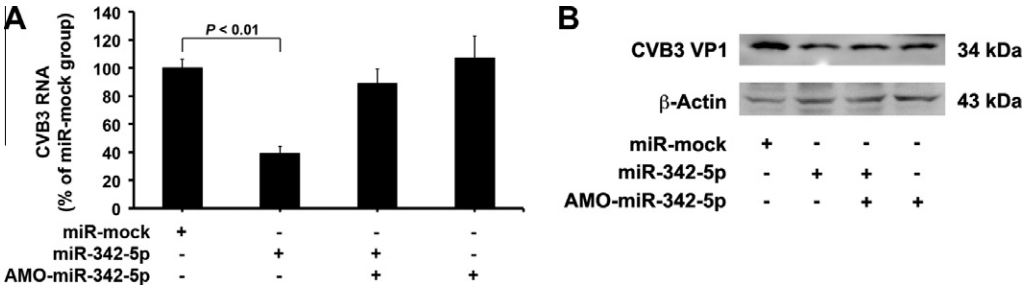

Fig. 4. Inhibitory effect of miR-342-5p on the biosynthesis of CVB3 wild type. Seventy percent confluent HeLa cells were transfected with miR-342-5p, AMO-miR-342-5p, and miR-mock, respectively, or co-transfected with miR-342-5p and AMO-miR-342-5p. The cells were infected with wild-type CVB3 (Woodruff strain) at 24 h post-transfection. (A) CVB3 RNA was quantified by RT-qPCR 24 h p.i. CVB3 RNA levels in the treated cells were normalized to the levels observed in miR-mock-treated cells. Results are presented as the mean ± s.d. ($n = 6$). (B) The proteins of the treated cells were extracted 24 h p.i. CVB3 VP1 was examined by Western blotting using an anti-enteroviral VP1 antibody.

counting EGFP-positive cells with a fluorescence microscope and measuring fluorescence intensity with a NanoDrop 3300. The pEGFP-C1 plasmid was employed as an EGFP gene expression control. The EGFP-positive cell count and fluorescence intensity in the cells co-transfected with pEGFP-C1 and miR-342-5p were almost identical to that observed in the cells transfected with pEGFP-C1 and miR-mock ($P > 0.05$, $n = 6$) (Fig. 5). Thus, miR-342-5p did not influence EGFP expression from the cassette itself.

Among the cells transfected with pEGFP-VP4-3, the proportion of EGFP-positive cells was 14.5% lower than that observed in the miR-mock-treated cells 32 h post-transfection ($P < 0.01$, $n = 6$). However, there was no significant difference between the fluorescence intensity levels of the two groups ($P > 0.05$, $n = 6$) (Fig. 5). Among the cells transfected with pEGFP-2C at the same time point, the EGFP-positive cell proportion of the miR-342-5p-treated cells was 65.9% lower than the proportion observed with the miR-mock-treated cells ($P < 0.01$, $n = 6$) (Fig. 5). The fluorescence intensity of miR-342-5p-treated cells was 43.5% lower than that of the miR-mock-treated cells ($P < 0.01$, $n = 6$) (Fig. 5). These results suggest that the miR-342-5p target is located in the 2C-coding region rather than VP2-coding region of CVB3.

There were two putative miR-342-5p targets in the 2C-coding region according to our predictions. To further identify the targets in the 2C-coding region, three mutated pEGFP-2C plasmids were generated via over-lapping PCR (Fig. 6A and Fig. S2): (1) in pEGFP-2C/m1, six nucleotides between nt4293–nt4321 were substituted, including U4294G, U4300C, C4303U, A4306G, G4309A, and C4318U; (2) in pEGFP-2C/m2, eight nucleotides between nt4989 and nt5015 were substituted, including C4990U, G4993A, C4996U, C5002U, G5005U, U5008G, C5011G, and U5014C; (3) in pEGFP-2C/m1 + m2, both the nt4293–nt4321 and nt4989–nt5015 sequences were mutated using the same substitutions of m1 and m2. As these mutations occurred in an open reading frame, only the third nucleotides of each codon was substituted. Therefore, the mutations significantly reduced the match quality of the putative targets to miR-342-5p but did not change the amino acid sequence of the translational products.

Using the same protocol as above, miR-342-5p or miR-mock were co-transfected into HeLa cells with pEGFP-2C/m1, pEGFP-2C/m2, pEGFP-2C/m1 + m2, and pEGFP-C1, respectively. EGFP expression in these cells was measured at 32 h post-transfection with a fluorescence microscope and spectrometer. Both the EGFP-positive cell counts and EGFP intensities in the pEGFP-2C- and pEGFP-2C/m1-transfected cells with miR-342-5p were significantly lower than the cells transfected with miR-mock ($n = 6$) (Fig. 6). However, miR-342-5p did not greatly suppress EGFP expression in pEGFP-2C/m2- and pEGFP-2C/m1 + m2-transfected cells ($n = 6$) (Fig. 6). These results demonstrate that mutations in the nt4293–nt4321 region did not affect the interaction between EGFP-2C and miR-342-5p, while mutations in the nt4989–nt5015 region greatly reduced the effect of miR-342-5p on EGFP-2C expression. Therefore, these data suggest miR-342-5p target is in the 2C-coding region and located in the nt4989–nt5015 but not the nt4293–nt4321 sequence.

3.6. MiR-342-5p also suppresses the biosynthesis in other CVBs

Alignment of the nt4989–nt5015 sequences of CVB type 1–5 indicates that this region, especially the region that matches with the seed sequence of miR-342-5p, is highly conserved in CVBs (Fig. 7A). Therefore, it is likely that miR-342-5p suppresses the biosynthesis of CVBs other than CVB3. To verify our speculation, VP1 protein expression of CVB1 and CVB5 in infected HeLa cells with miR-342-5p was examined using Western blotting with a monoclonal anti-enteroviral VP1 antibody. Interestingly, the VP1 levels of CVB1 and CVB5 were also inhibited by miR-342-5p in the infected cells, and the inhibition was reversed with treatment using AMO-miR-342-5p (Fig. 7B). These data indicate that the suppressive effect of miR-342-5p is not CVB type 3-specific and that the biosynthesis of other CVB types can be affected by miR-342-5p.

3.7. MiR-342-5p is differentially expressed in mouse organs

Balb/c mice are one of the most frequently used animals in CVB infection studies. To examine the possible impact of miR-342-5p on CVB3 infection *in vivo*, the miR-342-5p expression profile in various organs of Balb/c mice was examined. Total RNA was extracted from the organs of 2-week-old Balb/c mice, and RT-qPCR was performed to measure the abundance of miR-342-5p in these organs ($n = 6$). In addition, miR-133a levels were also determined to serve as a control for sample quality. The miR-133a expression profile in this study was consistent with a previous report (Tang et al., 2007). Our analysis indicated that miR-342-5p was expressed differentially in the organs of Balb/c mice. The lowest miR-342-5p abundance was found in liver, and the highest was observed in spleen (Fig. 8). A moderate miR-342-5p abundance was found in the gut, heart, and brain, all the main locations of CVB infection. These findings suggest that miR-342-5p, as one of the host factors, may be involved in the interaction between CVB3 infection and host innate antiviral defense *in vivo*.

4. Discussion

Given the ubiquitous impact of miRNAs on gene expression, it is evident that miRNAs play a critical role in the interaction between viruses and host cells (Ghosh et al., 2009; Grassmann and Jeang, 2008). On one hand, the cell may respond to viral infection by

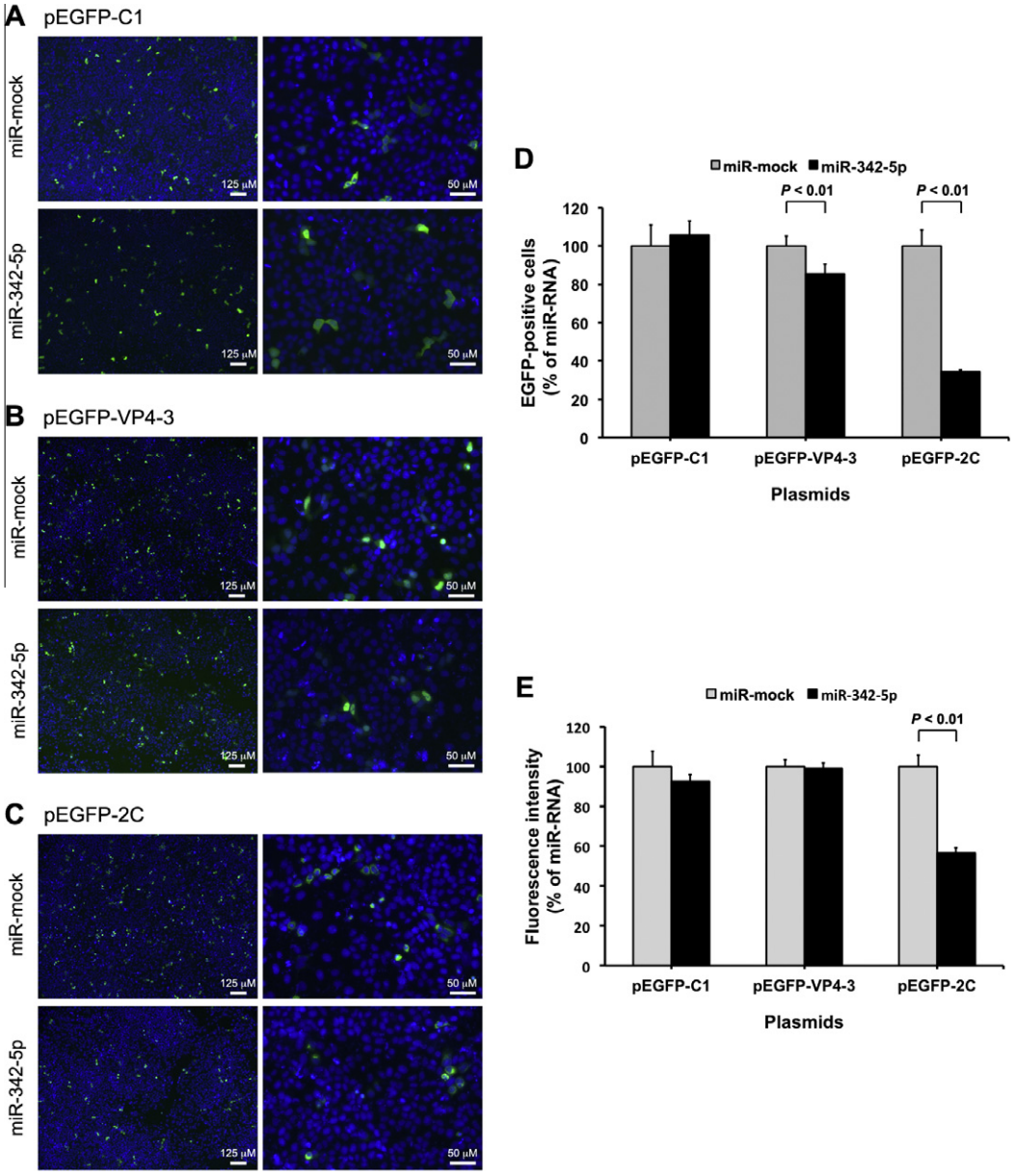

Fig. 5. Determination of miR-342-5p targets in the CVB3 genome. For the experiment, miR-342-5p or miR-mock were co-transfected into HeLa cells with pEGFP-VP4-3, pEGFP-2C, and pEGFP-C1, respectively. Hoechst 33342 was added into the culture medium to stain the nuclei at 24 h post-transfection. EGFP expression in these cells was analyzed at 32 h post-transfection. (A–C) EGFP expression in the transfected cells was observed with a fluorescent microscope. (D) EGFP-positive cells were counted with fluorescence microscope. The EGFP-positive cell counts were normalized to the number of nuclei in each sample. The relative counts of EGFP-positive cells of miR-342-5p-treated groups were calculated by normalizing to the miR-mock-treated groups ($n = 6$). (E) The fluorescence intensity of the cells was measured using a NanoDrop 3300. The EGFP intensity was normalized to the Hoechst 33342 intensity in each sample. The relative EGFP intensities of the miR-342-5p-treated groups were calculated by normalizing to the miR-mock-treated groups ($n = 6$). Error bars represent the s.d.

altering its miRNA expression profile (Lecellier et al., 2005; Song et al., 2010). On the other hand, some viruses, such as human immunodeficiency virus and hepatitis C virus, can take advantage of cellular miRNAs to facilitate viral survival and replication (Ghosh et al., 2009; Huang et al., 2007; Jopling et al., 2005). CVBs belong to the Enterovirus genus of the *Picornaviridae* family and have positive single-stranded RNA (Kawai, 1999). CVBs genomes are essentially the same as mRNAs and can directly guide viral biosynthesis in host cells (Esfandiarei and McManus, 2008). Therefore, they are very likely to be directly modulated by cellular miRNAs.

MiR-342-5p [miRBase: MIMAT0004694 (human), MIMAT0004653 (mouse)] is a mature form of miR-342 that is coded by chromosome 14 in humans (chr14:99645745–99645843) and chromosome 12 in mice (chr12:109106427–109106525) (Landgraf et al., 2007). In addition, miR-342 plays a role in the inhibition of colorectal cancer cell proliferation and invasion by directly targeting DNA methyltransferase 1 (Wang et al., 2011). Expression of miR-342 is downregulated in tamoxifen-resistant breast cancer cells and may be involved in tamoxifen-mediated tumor cell apoptosis and cell cycle progression (Cittelly et al., 2010). However, the full role of miR-342-5p in cellular biology and pathogenesis is unknown. A genome-wide miRNA profiling study with peripheral blood leukocytes demonstrated that miR-342-5p expression in sepsis patients was downregulated compared to healthy controls, but its biological influence has not been investigated (Vasilescu et al., 2009).

In this study, by screening the possible interaction between the CVB3 genome and various miRNAs, we found that there were

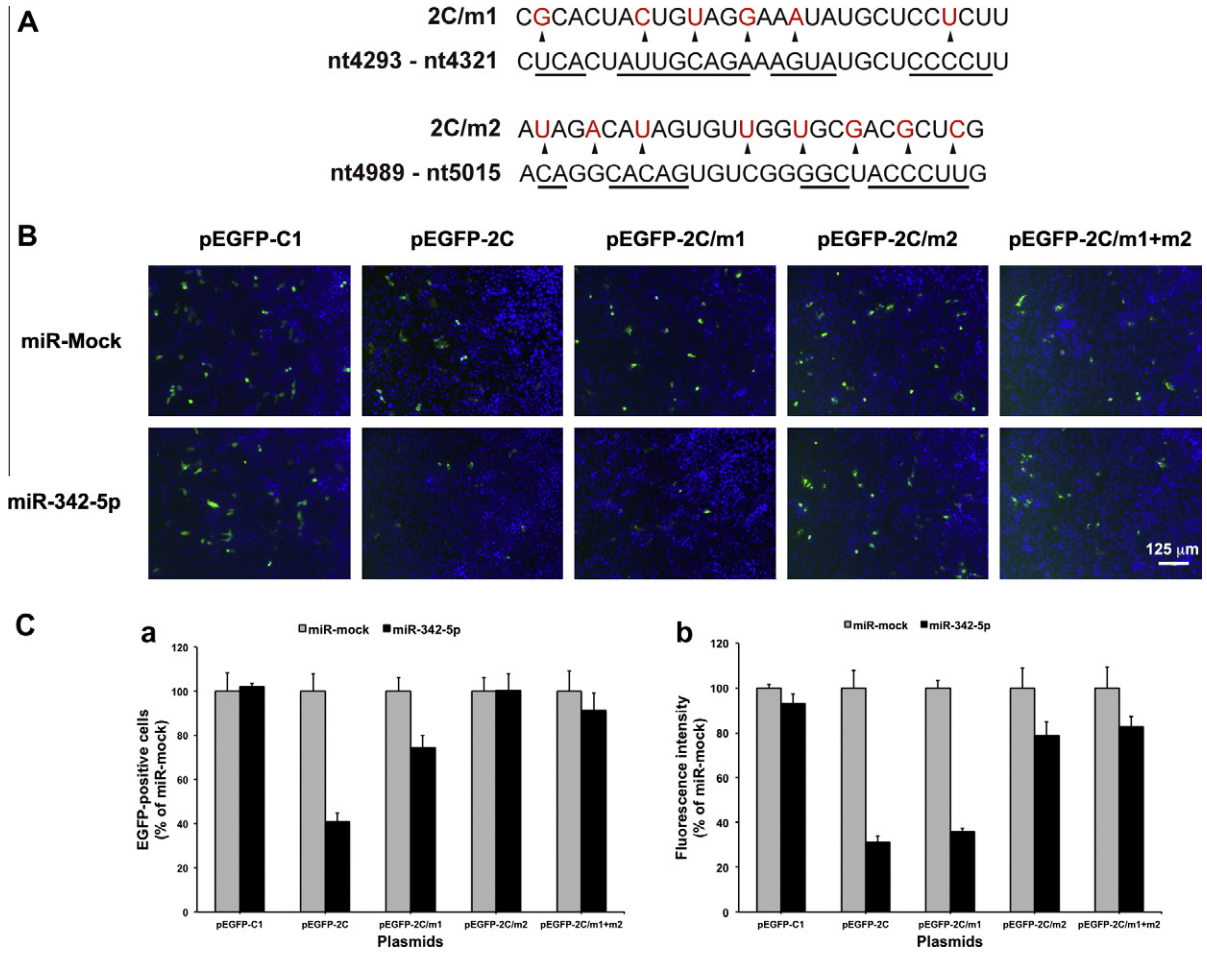

Fig. 6. Identification of miR-342-5p targets in the 2C-coding region of CVB3 genome. (A) Three mutated pEGFP-2C were generated by over-lapping PCR to reduce the match of the putative targets in the 2C-coding region to miR-243-5p: (1) 2C/m1: six nucleotides at nt4293–nt4321 were mutated; (2) 2C/m2: eight nucleotides at nt4989–nt5015 were mutated; (3) 2C/m1 + m2: both nt4293–nt4321 and nt4989–nt5015 were mutated by the same strategies used in m1 and m2. Only the third nucleotides of the codons were mutated. (B) MiR-342-5p or miR-mock were co-transfected into HeLa cells with pEGFP-2C/m1, pEGFP-2C/m2, pEGFP-2C/m1 + m2, and pEGFP-C1, respectively. Hoechst 33342 was added into the culture medium to stain the nuclei at 24 h post-transfection. EGFP expression in the treated cells was observed at 32 h post-transfection with a fluorescence microscope. (C) EGFP-positive cell counts (a) and EGFP fluorescence intensity (b) in the treated cells were measured as in Fig. 5. Error bars represent the s.d. (n = 6).

potential miR-342-5p targets in the CVB3 genome. *In vitro* studies verified that the biosynthesis of CVB3 could be significantly inhibited by miR-342-5p, and the target of miR-342-5p was located in the 2C-coding region of the CVB3 genome. Therefore, as a host factor, miR-342-5p may play a role in the innate defense against CVB3 infection.

By screening the genome of CVB3 for potential targets of various miRNAs with RNAhybrid 2.2 and miRanda 3.2a, we found three possible target sites of miR-342-5p located in the 2C- and VP2-coding regions of the CVB3 genome. To verify these predictions, two CVB3 variants that had the reporter genes RLuc and EGFP, respectively, in their genome were used to examine the effects of miR-342-5p on CVB3 biosynthesis. RLuc expression was significantly suppressed in the RLuc-CVB3-infected HeLa cells with miR-342-5p, but other randomly selected miRNAs had no significant effect on RLuc-CVB3. Similarly, EGFP expression was significantly suppressed in EGFP-CVB3-infected HeLa cells with miR-342-5p, and the inhibitory effect of miR-342-5p could be reversed by AMO-miR-342-5p. These data indicate that miR-342-5p can specifically suppress CVB3 biosynthesis.

RLuc-CVB3 and EGFP-CVB3 are genetically engineered CVB3 variants. To exclude the bias originating from the artificial modification in viral genome, wild-type CVB3 was also examined to evaluate the effect of miR-342-5p. The CVB3 genomic RNA expression level and VP1 protein level were significantly downregulated in the infected cells transfected with miR-342-5p, and the downregulation could be reversed by AMO-miR-342-5p. These results were consistent with the results obtained using the reporter gene CVB3 variants. Taken together, these data indicate miR-342-5p can downregulate both the protein and RNA synthesis of CVB3. In either case, CVB3 replication could be inhibited.

To validate the predicted targets of miR-342-5p in the CVB3 genome, we tried to construct CVB3 variants with mutations in the putative target sites using a site-directed mutagenesis strategy. These mutations resulted in virulence loss and even a complete loss of infectivity (data not shown). Picornavirus genomes are very sensitive to modifications. A substitution of a single nucleotide or the insertion of a reporter gene can dramatically change the phenotype and genomic stability of CVBs (Tong et al., 2011; Zhong et al., 2008). Therefore, we chose an alternate strategy over mutagenesis in the full-length genome to identify the targets. Plasmids expressing EGFP-VP4-3 and EGFP-2C were generated. By quantitating the EGFP-positive cells and green fluorescence intensity, we found miR-342-5p did not significantly affect the expression of EGFP (pEGFP-C1) and EGFP-VP4-3. However, miR-342-5p could significantly suppress the expression of EGFP-2C. These data indicate that the target of miR-342-5p was located in the 2C-coding region rather than the VP2-coding region.

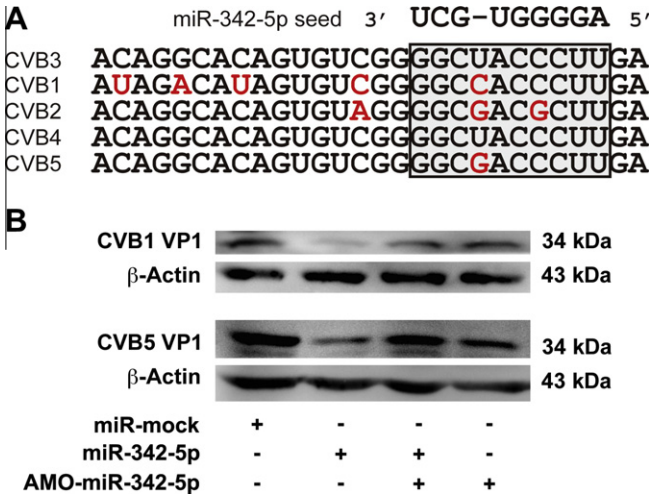

Fig. 7. Effect of miR-342-5p on other types of CVBs. (A) Alignment of the nt4989–nt5015 sequences of CVB type 1–5 [GenBank accession: M16560 (CVB1), AF081485 (CVB2), U57056 (CVB3), X05690 (CVB4), X67706 (CVB5)]. The mismatched nucleotides are marked in red. The viral sequences that match with the seed sequence of miR-342-5p are framed in the gray box. (B) The expression of the VP1 proteins of CVB1 and CVB5 in HeLa cells with miR-342-5p and/or AMO-miR-342-5p. The cells were transfected with miR-342-5p, miR-mock, AMO-miR-342-5p, respectively, or co-transfected with miR-342-5p and AMO-miR-342-5p. The transfected cells were infected with CVB1 or CVB5 (MOI = 0.01) at 24 h post-transfection. The cellular proteins were extracted and examined at 24 h p.i. by Western blotting using an anti-enteroviral VP1 antibody. (For interpretation of the references to color in this figure legend, the reader is referred to the web version of this article.)

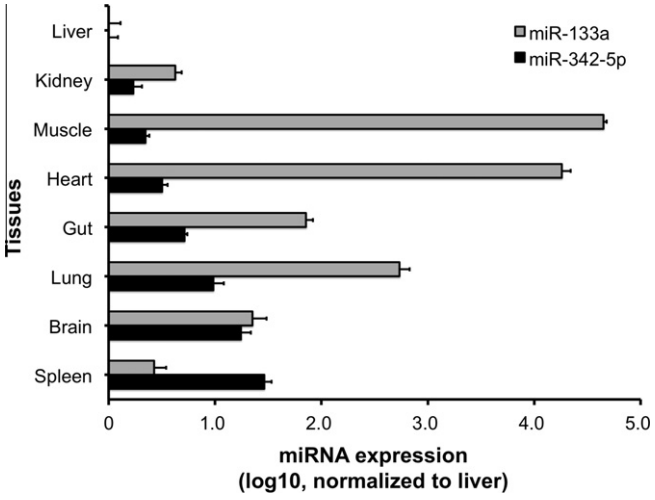

Fig. 8. MiR-342-5p expression profile in various organs of Balb/c mouse. The organs of 2-week-old healthy Balb/c mice ($n = 6$) were collected under anesthetic conditions. The total RNA of these tissues was extracted with TRIzol. The miR-342-5p and miR-133a levels were measured by RT-qPCR. U6 snRNA was used to normalize the abundance of miRNAs in each sample. The relative abundances of miRNAs in various organs were calculated by normalizing them with that in the liver. Error bars represent the s.d.

According to our predictions, there are two putative miR-342-5p target sites in the 2C-coding region. To determine which was the actual miR-342-5p target, we generated three mutated pEGFP-2C plasmids (pEGFP-2C/m1, pEGFP-2C/m2, and pEGFP-2C/m1 + m2). All the mutations only reduced the proportion of matching with the miR-342-5p sequence but did not change its amino acid coding. By monitoring EGFP expression, mutations between nt4293 and nt4321 did not affect the suppression of EGFP-2C expression by miR-342-5p, while mutations between nt4989 and nt5015 significantly reduced the influence of miR-342-5p on the expression of EGFP-2C. These data demonstrate that miR-342-5p suppresses CVB3 biosynthesis through the interaction with the nt4989–nt5015 sequence in CVB3 genome. However, it is possible that there may be other targets of miR-342-5p in the CVB3 genome that were not recognized by the prediction tools. The above-described screening strategy may find new miR-342-5p targets in the CVB3 genome.

An interesting question is whether miR-342-5p can interact with other types of CVBs besides CVB3. The sequence alignment of nt4989–nt5015 with CVB types 1–5 indicates that this region, especially the region complementary to the miR-342-5p seed sequence, is highly conserved among these types. When we examined the VP1 expression levels of CVB1 and CVB5 with Western blotting, we observed that miR-342-5p could effectively inhibit the expression of VP1 proteins of CVB1 and CVB5. Therefore, it is very likely that miR-342-5p may exert its suppressive effects to other CVB types as well.

miRNAs function through imperfect complementary binding to their target sequence in mRNA of animal cells (Ambros, 2004; Asli et al., 2008; Bartel, 2004). These characteristics of miRNAs allow each miRNA to potentially target multiple mRNAs (Lewis et al., 2005; Lim et al., 2005). Although our data demonstrate that miR-342-5p inhibits CVB3 replication by directly targeting the 2C-coding region of CVB3 genome, we cannot exclude the possibility that miR-342-5p may also regulate the expression of certain cellular genes and thereafter indirectly modulate CVB3 infection.

In the present study, we found that miR-342-5p was moderately expressed in the gut, heart, and brain of healthy Balb/c mice (Fig. 8). The gut, heart, and brain are organs most involved with CVB infection (Vargova et al., 2003). The moderate abundance of miR-342-5p in these organs allow an opportunity for CVB3 to encounter and be modulated by miR-342-5p when it invades these organs. CVB3 must overcome the adverse effects of miR-342-5p on its biosynthesis to facilitate its replication and infection. It is unknown whether miR-342-5p expression is altered in these organs when CVB3 infection occurs. Previous studies have shown that virus infection often alters the host miRNA profile (Houzet et al., 2008; Li et al., 2010; Wald et al., 2011). Therefore, further *in vivo* studies may help us to understand the reciprocal impact of CVB3 infection and miR-342-5p expression.

Previous studies have indicated that the antiviral potential of certain miRNAs might be employed as therapeutic approaches in the treatment of viral diseases (Kurzynska-Kokorniak et al., 2009; Nunnari and Schnell, 2011; Sakurai et al., 2011; Sall et al., 2008). In accordance with those studies, this study suggests that miR-342-5p may be a candidate miRNA for use in the treatment of CVBs-related diseases such as myocarditis, cardiomyopathy, and encephalitis. *In vivo* studies with synthesized miR-342-5p or miR-342-5p-expressing vectors will be helpful in evaluating the therapeutic value of miR-342-5p.

Conflict of interest

We declare that there are no conflicts of interest among the authors.

Acknowledgments

This work was supported by Natural Science Foundation of China (NSFC) Grants to Z. Zhong (No. 30872231) and L. Tong (No. 81101234). We are grateful to Dr. Xiaoning Si, Ph.D. of Carestream Molecular Imaging (China) for his constructive suggestions. We also thank the Heilongjiang Provincial Key Laboratory of Pathogens and Immunity, Harbin 150081, China, for laboratory and technical support.

Appendix A. Supplementary data

Supplementary data associated with this article can be found, in the online version, at doi:10.1016/j.antiviral.2011.12.004.

References

Alves Jr., L., Niemeier, S., Hauenschild, A., Rehmsmeier, M., Merkle, T., 2009. Comprehensive prediction of novel microRNA targets in *Arabidopsis thaliana*. Nucleic Acids Res. 37, 4010–4021.

Ambros, V., 2004. The functions of animal microRNAs. Nature 431, 350–355.

Asli, N.S., Pitulescu, M.E., Kessel, M., 2008. MicroRNAs in organogenesis and disease. Curr. Mol. Med. 8, 698–710.

Bartel, D.P., 2004. MicroRNAs: genomics, biogenesis, mechanism, and function. Cell 116, 281–297.

Bedard, K.M., Semler, B.L., 2004. Regulation of picornavirus gene expression. Microbes Infect. 6, 702–713.

Bowles, N.E., Richardson, P.J., Olsen, E.G., Archard, L.C., 1986. Detection of coxsackie-B-virus-specific RNA sequences in myocardial biopsy samples from patients with myocarditis and dilated cardiomyopathy. Lancet 1, 1120–1123.

Cittelly, D.M., Das, P.M., Spoelstra, N.S., Edgerton, S.M., Richer, J.K., Thor, A.D., Jones, F.E., 2010. Downregulation of miR-342 is associated with tamoxifen resistant breast tumors. Mol. Cancer 9, 317.

Cui, A., Yu, D., Zhu, Z., Meng, L., Li, H., Liu, J., Liu, G., Mao, N., Xu, W., 2010a. An outbreak of aseptic meningitis caused by coxsackievirus A9 in Gansu, the People's Republic of China. Virol. J. 7, 72.

Cui, L., Guo, X., Qi, Y., Qi, X., Ge, Y., Shi, Z., Wu, T., Shan, J., Shan, Y., Zhu, Z., Wang, H., 2010b. Identification of microRNAs involved in the host response to enterovirus 71 infection by a deep sequencing approach. J. Biomed. Biotechnol. 2010, 425939.

Esfandiarei, M., McManus, B.M., 2008. Molecular biology and pathogenesis of viral myocarditis. Annu. Rev. Pathol. 3, 127–155.

Esquela-Kerscher, A., Slack, F.J., 2006. Oncomirs – microRNAs with a role in cancer. Nat. Rev. Cancer 6, 259–269.

Feuer, R., Mena, I., Pagarigan, R., Slifka, M.K., Whitton, J.L., 2002. Cell cycle status affects coxsackievirus replication, persistence, and reactivation in vitro. J. Virol. 76, 4430–4440.

Ghosh, Z., Mallick, B., Chakrabarti, J., 2009. Cellular versus viral microRNAs in host–virus interaction. Nucleic Acids Res. 37, 1035–1048.

Grassmann, R., Jeang, K.T., 2008. The roles of microRNAs in mammalian virus infection. Biochim. Biophys. Acta 1779, 706–711.

Ho, B.C., Yu, S.L., Chen, J.J., Chang, S.Y., Yan, B.S., Hong, Q.S., Singh, S., Kao, C.L., Chen, H.Y., Su, K.Y., Li, K.C., Cheng, C.L., Cheng, H.W., Lee, J.Y., Lee, C.N., Yang, P.C., 2011. Enterovirus-induced miR-141 contributes to shutoff of host protein translation by targeting the translation initiation factor eIF4E. Cell Host Microbe 9, 58–69.

Houzet, L., Yeung, M.L., de Lame, V., Desai, D., Smith, S.M., Jeang, K.T., 2008. MicroRNA profile changes in human immunodeficiency virus type 1 (HIV-1) seropositive individuals. Retrovirology 5, 118.

Huang, J., Wang, F., Argyris, E., Chen, K., Liang, Z., Tian, H., Huang, W., Squires, K., Verlinghieri, G., Zhang, H., 2007. Cellular microRNAs contribute to HIV-1 latency in resting primary CD4+ T lymphocytes. Nat. Med. 13, 1241–1247.

Jiang, J., Gusev, Y., Aderca, I., Mettler, T.A., Nagorney, D.M., Brackett, D.J., Roberts, L.R., Schmittgen, T.D., 2008. Association of MicroRNA expression in hepatocellular carcinomas with hepatitis infection, cirrhosis, and patient survival. Clin. Cancer Res. 14, 419–427.

Jin, O., Sole, M.J., Butany, J.W., Chia, W.K., McLaughlin, P.R., Liu, P., Liew, C.C., 1990. Detection of enterovirus RNA in myocardial biopsies from patients with myocarditis and cardiomyopathy using gene amplification by polymerase chain reaction. Circulation 82, 8–16.

Jopling, C.L., Yi, M.K., Lancaster, A.M., Lemon, S.M., Sarnow, P., 2005. Modulation of hepatitis C virus RNA abundance by a liver-specific MicroRNA. Science 309, 1577.

Kawai, C., 1999. From myocarditis to cardiomyopathy: mechanisms of inflammation and cell death: learning from the past for the future. Circulation 99, 1091.

Kelly, E.J., Hadac, E.M., Cullen, B.R., Russell, S.J., 2010. MicroRNA antagonism of the picornaviral life cycle: alternative mechanisms of interference. PLoS Pathog. 6, e1000820.

Kloosterman, W.P., Plasterk, R.H., 2006. The diverse functions of microRNAs in animal development and disease. Dev. Cell 11, 441–450.

Knowlton, K.U., 2008. CVB infection and mechanisms of viral cardiomyopathy. Curr. Top. Microbiol. Immunol. 323, 315–335.

Kurzynska-Kokorniak, A., Jackowiak, P., Figlerowicz, M., 2009. Human- and virus-encoded microRNAs as potential targets of antiviral therapy. Mini Rev. Med. Chem. 9, 927–937.

Landgraf, P., Rusu, M., Sheridan, R., Sewer, A., Iovino, N., Aravin, A., Pfeffer, S., Rice, A., Kamphorst, A.O., Landthaler, M., Lin, C., Socci, N.D., Hermida, L., Fulci, V., Chiaretti, S., Foa, R., Schliwka, J., Fuchs, U., Novosel, A., Muller, R.U., Schermer, B., Bissels, U., Inman, J., Phan, Q., Chien, M., Weir, D.B., Choksi, R., De Vita, G., Frezzetti, D., Trompeter, H.I., Hornung, V., Teng, G., Hartmann, G., Palkovits, M., Di Lauro, R., Wernet, P., Macino, G., Rogler, C.E., Nagle, J.W., Ju, J., Papavasiliou, F.N., Benzing, T., Lichter, P., Tam, W., Brownstein, M.J., Bosio, A., Borkhardt, A., Russo, Sander, C., Zavolan, M., Tuschl, T., . A mammalian microRNA expression atlas based on small RNA library sequencing. Cell 129, 1401–1414.

Lecellier, C.H., Dunoyer, P., Arar, K., Lehmann-Che, J., Eyquem, S., Himber, C., Saïb, A., Voinnet, O., 2005. A cellular microRNA mediates antiviral defense in human cells. Science 308, 557.

Lewis, B.P., Burge, C.B., Bartel, D.P., 2005. Conserved seed pairing, often flanked by adenosines, indicates that thousands of human genes are microRNA targets. Cell 120, 15–20.

Li, L.M., Hu, Z.B., Zhou, Z.X., Chen, X., Liu, F.Y., Zhang, J.F., Shen, H.B., Zhang, C.Y., Zen, K., 2010. Serum microRNA profiles serve as novel biomarkers for HBV infection and diagnosis of HBV-positive hepatocarcinoma. Cancer Res. 70, 9798–9807.

Lim, L.P., Lau, N.C., Garrett-Engele, P., Grimson, A., Schelter, J.M., Castle, J., Bartel, D.P., Linsley, P.S., Johnson, J.M., 2005. Microarray analysis shows that some microRNAs downregulate large numbers of target mRNAs. Nature 433, 769–773.

Livak, K.J., Schmittgen, T.D., 2001. Analysis of relative gene expression data using real-time quantitative PCR and the 2(−Delta Delta C(T)) method. Methods 25, 402–408.

Ma, L., Liu, J., Shen, J., Liu, L., Wu, J., Li, W., Luo, J., Chen, Q., Qian, C., 2010. Expression of miR-122 mediated by adenoviral vector induces apoptosis and cell cycle arrest of cancer cells. Cancer Biol. Ther. 9, 554–561.

Martin, A.B., Webber, S., Fricker, F.J., Jaffe, R., Demmler, G., Kearney, D., Zhang, Y.H., Bodurtha, J., Gelb, B., Ni, J., 1994. Acute myocarditis. Rapid diagnosis by PCR in children. Circulation 90, 330–339.

Nunnari, G., Schnell, M.J., 2011. MicroRNA-122: a therapeutic target for hepatitis C virus (HCV) infection. Front. Biosci. (Schol. Ed.) 3, 1032–1037.

Pedersen, I.M., Cheng, G., Wieland, S., Volinia, S., Croce, C.M., Chisari, F.V., David, M., 2007. Interferon modulation of cellular microRNAs as an antiviral mechanism. Nature 449, 919.

Rajewsky, N., 2006. MicroRNA target predictions in animals. Nat. Genet. 38 (Suppl.), S8–S13.

Sakurai, F., Katayama, K., Mizuguchi, H., 2011. MicroRNA-regulated transgene expression systems for gene therapy and virotherapy. Front. Biosci. 17, 2389–2401.

Sall, A., Liu, Z., Zhang, H.M., Yuan, J., Lim, T., Su, Y., Yang, D., 2008. MicroRNAs-based therapeutic strategy for virally induced diseases. Curr. Drug Discov. Technol. 5, 49–58.

Schmittgen, T.D., Jiang, J., Liu, Q., Yang, L., 2004. A high-throughput method to monitor the expression of microRNA precursors. Nucleic Acids Res. 32, e43.

Song, L., Liu, H., Gao, S., Jiang, W., Huang, W., 2010. Cellular microRNAs inhibit replication of the H1N1 influenza A virus in infected cells. J. Virol. 84, 8849–8860.

Sullivan, C.S., Ganem, D., 2005. MicroRNAs and viral infection. Mol. Cell 20, 3–7.

Tang, X., Gal, J., Zhuang, X., Wang, W., Zhu, H., Tang, G., 2007. A simple array platform for microRNA analysis and its application in mouse tissues. RNA 13, 1803–1822.

Tong, L., Lin, L., Zhao, W., Wang, B., Wu, S., Liu, H., Zhong, X., Cui, Y., Gu, H., Zhang, F., Zhong, Z., 2011. Destabilization of coxsackievirus B3 genome integrated with enhanced green fluorescent protein gene. Intervirology 54, 268–275.

Tracy, S., Chapman, N.M., McManus, B.M., Pallansch, M.A., Beck, M.A., Carstens, J., 1990. A molecular and serologic evaluation of enteroviral involvement in human myocarditis. J. Mol. Cell. Cardiol. 22, 403–414.

Vargova, A., Bopegamage, S., Borsanyiova, M., Petrovicova, A., Benkovicova, M., 2003. Coxsackievirus infection of mice. II. Viral kinetics and histopathological changes in mice experimentally infected with coxsackievirus B3 by intraperitoneal route. Acta Virol. 47, 253–257.

Vasilescu, C., Rossi, S., Shimizu, M., Tudor, S., Veronese, A., Ferracin, M., Nicoloso, M.S., Barbarotto, E., Popa, M., Stanciulea, O., Fernandez, M.H., Tulbure, D., Bueso-Ramos, C.E., Negrini, M., Calin, G.A., 2009. MicroRNA fingerprints identify miR-150 as a plasma prognostic marker in patients with sepsis. PLoS ONE 4, e7405.

Verma, N.A., Zheng, X.T., Harris, M.U., Cadichon, S.B., Melin-Aldana, H., Khetsuriani, N., Oberste, M.S., Shulman, S.T., 2009. Outbreak of life-threatening coxsackievirus B1 myocarditis in neonates. Clin. Infect. Dis. 49, 759–763.

Wald, A.I., Hoskins, E.E., Wells, S.I., Ferris, R.L., Khan, S.A., 2011. Alteration of microRNA profiles in squamous cell carcinoma of the head and neck cell lines by human papillomavirus. Head Neck 33, 504–512.

Wang, H., Wu, J., Meng, X., Ying, X., Zuo, Y., Liu, R., Pan, Z., Kang, T., Huang, W., 2011. MicroRNA-342 inhibits colorectal cancer cell proliferation and invasion by directly targeting DNA methyltransferase 1. Carcinogenesis 32, 1033–1042.

Weiler, J., Hunziker, J., Hall, J., 2006. Anti-miRNA oligonucleotides (AMOs): ammunition to target miRNAs implicated in human disease? Gene Ther. 13, 496–502.

Wong, A.H., Lau, C.S., Cheng, P.K., Ng, A.Y., Lim, W.W., 2011. Coxsackievirus B3-associated aseptic meningitis: an emerging infection in Hong Kong. J. Med. Virol. 83, 483–489.

Wu, X., Wu, S., Tong, L., Luan, T., Lin, L., Lu, S., Zhao, W., Ma, Q., Liu, H., Zhong, Z., 2009. MiR-122 affects the viability and apoptosis of hepatocellular carcinoma cells. Scand. J. Gastroenterol. 44, 1332–1339.

Yuan, J., Cheung, P.K., Zhang, H., Chau, D., Yanagawa, B., Cheung, C., Luo, H., Wang, Y., Suarez, A., McManus, B.M., Yang, D., 2004. A phosphorothioate antisense oligodeoxynucleotide specifically inhibits coxsackievirus B3 replication in cardiomyocytes and mouse hearts. Lab. Invest. 84, 703–714.

Zhong, Z., Li, X., Zhao, W., Tong, L., Liu, J., Wu, S., Lin, L., Zhang, Z., Tian, Y., Zhang, F., 2008. Mutations at nucleotides 573 and 579 within 5′-untranslated region augment the virulence of coxsackievirus B1. Virus Res. 135, 255–259.